

Kardar-Parisi-Zhang universality in the phase distributions of one-dimensional exciton-polaritons

Davide Squizzato, Léonie Canet, and Anna Minguzzi
Univ. Grenoble Alpes and CNRS, LPMMC, F-38000 Grenoble

Exciton-polaritons under driven-dissipative conditions exhibit a condensation transition which belongs to a different universality class than equilibrium Bose-Einstein condensates. By numerically solving the generalized Gross-Pitaevskii equation with realistic experimental parameters, we show that one-dimensional exciton-polaritons display fine features of Kardar-Parisi-Zhang (KPZ) dynamics. Beyond the scaling exponents, we show that their phase distribution follows the Tracy-Widom form predicted for KPZ growing interfaces. We moreover evidence a crossover to the stationary Baik-Rains statistics. We finally show that these features are unaffected on a certain timescale by the presence of a smooth disorder often present in experimental setups.

PACS numbers: 71.36.+c, 64.60.Ht, 89.75.Da, 02.50.-r

Non-equilibrium systems exhibit a large variety of critical behaviors, some of which having no counter-parts in equilibrium systems. This is the case for generic scale invariance, or self-organized criticality, which is realized for instance in the celebrated Kardar-Parisi-Zhang equation [1]. Originally derived to describe the kinetic roughening of growing interfaces, it arises in connection with an extremely large class of non-equilibrium or disordered systems [2, 3] and has therefore become a paradigmatic model in physics for non-equilibrium scaling and phase transitions, and an archetype in mathematics of stochastic processes with non-Gaussian statistics [4].

Recently, KPZ dynamics has been unveiled in a condensed matter system, the exciton-polariton condensate [5–10]. Exciton-polaritons (EP) are elementary excitations arising in a semiconductor microcavity coupled to cavity photons. Since EP have a finite lifetime, a stationary state is obtained under pumping. In these driven-dissipative conditions, the EP gas exhibits a non-equilibrium Bose-Einstein condensation transition, whose properties are intensively investigated [11]. It was shown that in a certain regime, the dynamics of the phase of the condensate can be mapped onto a KPZ equation. Whereas this finding was confirmed numerically in one dimension (1D) for well-chosen parameters [7], it was also suggested that this regime may not be accessible in current experimental systems.

In this paper, we re-examine the experimental realizability of KPZ universality in the 1D EP condensate. For this, we accurately model the system, taking into account realistic momentum-dependent losses and the quartic part of the dispersion of the polaritons. From this model, with actual experimental parameters, we numerically demonstrate that KPZ physics is observable under current experimental conditions. Moreover, beyond the KPZ scaling, we show that advanced KPZ properties can be accessed in this system, considering in particular the statistics of the phase fluctuations.

Indeed, a breakthrough in the understanding of the statistical properties of a 1D KPZ interface was achieved

since 2010, with the derivation of the exact distributions of the fluctuations of the height of the interface, followed by other exact results for the two-point correlations [4]. These advances highlighted remarkable features of the KPZ universality class: an unexpected connection with random matrix theory, with the appearance of Tracy-Widom (TW) distributions [12], which are the distributions of the largest eigenvalues of matrices in the gaussian orthogonal (GOE) or unitary ensemble (GUE). It was shown that the interface is sensitive to the global geometry, or equivalently to the initial conditions, defining three sub-classes differing by their statistics: TW-GOE for flat [13, 14], TW-GUE for sharp-wedge (*i.e.* delta-like) [15–17], or Baik-Rains (BR) distribution for stationary (*i.e.* Brownian) [18, 19] initial conditions, while sharing the same KPZ scaling exponents.

This geometry-dependent universal behavior was first observed experimentally in turbulent liquid crystal [20, 21]. However, despite recent progress, experimental observations of KPZ universality are still scarce [22, 23]. We show that the EP system stands as a promising candidate. We numerically study the fluctuations of the phase of the EP condensate, and show that they precisely follow a TW-GOE distribution. Moreover, we show that a crossover between the TW-GOE distribution and the BR one can be observed. This crossover is expected in a finite-size system when the correlations become comparable with the system size but before finite-size effects begin to dominate, and is very difficult to access [24]. We show clear signatures of this crossover in the numerical distributions. Finally, we investigate the effect of disorder, which is unavoidable in experimental systems, and show that KPZ physics is unaltered on a timescale related to the typical lengthscale of the disorder.

Model – A mean-field description of EP under incoherent pumping was introduced in [25]. In this description, the dynamics of the polariton condensate wavefunction ϕ is

given by

$$i\partial_t\phi = \left[\mathcal{F}^{-1} [E_{LP}(k)](x) + \frac{i}{2} (Rn_r - \gamma_l) + g|\phi|^2 \right] \phi, \quad (1)$$

where the polaritonic reservoir density n_r is determined by the rate equation

$$\partial_t n_r = P - \gamma_r n_r - Rn_r |\phi|^2. \quad (2)$$

$E_{LP}(k)$ is the lower-polariton dispersion in momentum space, \mathcal{F}^{-1} denoting the inverse Fourier transform, P is the pump, R the amplification term, γ_l the polariton loss rate, g the polariton-polariton interaction strength, and γ_r the reservoir loss rate. In the phenomenological model (1), the dispersion is usually approximated by a parabola of effective mass m_{LP} with momentum-independent loss-rate γ_l . In this work, in order to describe more accurately the experiments, we also include quartic corrections to this dispersion [11] $E_{LP}(k) \simeq \frac{\hbar^2 k^2}{2m_{LP}} - \frac{1}{2\Omega} \left(\frac{\hbar^2 k^2}{2m_{LP}} \right)^2$, together with a momentum-dependent loss-rate $\gamma(k) = \gamma_l + \gamma^{(2)}k^2$, which originates from localized exciton reservoirs. These two effects result in an imaginary diffusion coefficient in the dynamics of the condensate, whose presence turns out to be crucial (see below).

In the case where the time scales in the reservoir and in the condensate are well separated, one can solve the dynamics of the reservoir density to obtain an effective equation for the polaritonic condensate, which in dimensionless form reads

$$i\partial_t\phi = [-(1 - iK_d)\nabla^2 - K_c^{(2)}\nabla^4 - (r_c - ir_d) + (u_c - iu_d)|\phi|^2] \phi + \sqrt{\sigma}\xi, \quad (3)$$

where we rescaled the time in units of $\bar{t} = \gamma_l^{-1}$, the space in units of $\bar{x} = (\hbar/2m_{LP}\gamma_l)^{1/2}$ and the condensate wavefunction in units of $\bar{\phi} = (\gamma_r(p-1)/Rp)^{1/2}$ with $p = PR/(\gamma_l\gamma_r)$. The parameters in (3) are related to the parameters of the microscopic model *via* $r_d = u_d = (p-1)/2$, $u_c = \gamma_r g(p-1)/(R\gamma_l p)$, $\sigma = Rp(p+1)/(2x^*\gamma_r(p-1))$, and r_c determined from the stationary-homogeneous solution of (3). The stochastic noise $\xi(x, t)$, with $\langle \xi(x, t)\xi^*(x', t') \rangle = 2\delta(x-x')\delta(t-t')$ originates from the driven-dissipative nature of the fluid [26, 27]. Equation (3) is a generalized Gross-Pitaevskii Equation (gGPE) with complex coefficients.

KPZ mapping – As shown in [10], by expressing the condensate wavefunction in a density-phase representation $\phi(x, t) = \sqrt{\rho(x, t)} \exp(i\theta(x, t))$ and performing a mean-field approximation over the density ρ at the level of the Keldysh action for the EP, one obtains that the dynamics of the phase field θ is ruled by the KPZ equation

$$\partial_t\theta = \nu\nabla^2\theta + \frac{\lambda}{2}(\nabla\theta)^2 + \sqrt{D}\eta, \quad (4)$$

where η is a white noise with $\langle \eta(x, t)\eta(x', t') \rangle = 2\delta(x-x')\delta(t-t')$ and $\nu = (K_c u_c/u_d + K_d)$, $\lambda = -2(K_c -$

$K_d u_c/u_d)$, $D = \sigma u_d (1 + u_c^2/u_d^2)/2r_d$ [8]. The original KPZ equation describes the dynamics of the height of a stochastically growing interface. A 1D interface always roughens: it generically becomes scale-invariant. Its profile can be characterized by the roughness, defined in term of θ as $w^2(L, t) = \langle \theta^2(x, t) - \langle \theta(x, t) \rangle_x^2 \rangle_{\xi, x}$, where $\langle \cdot \rangle_x = 1/L \int_x \cdot$ is the spatial average and $\langle \cdot \rangle_{\xi}$ the average over different realizations of the noise. The KPZ roughness is known to endow the Family-Vicsek scaling form [2, 28]

$$w(L, t) \sim t^\beta F(Lt^{-1/z}) \sim \begin{cases} t^\beta, & t < T_s \\ L^\chi, & t > T_s \end{cases} \quad (5)$$

with $T_s \sim L^z$, and where the critical exponents take the exact values $\chi = 1/2$ and $z = 3/2$, $\beta = \chi/z = 1/3$ for the 1D KPZ universality class.

Numerical simulations – We numerically integrate the gGPE (3) using standard Monte Carlo sampling of the noise [29, 30]. The parameters in this equation depend on the material. We use values typical for CdTe, used *e.g.* in Grenoble experiments: $m_{LP} = 4 \times 10^{-5} m_e$, $\gamma_l = 0.5 \text{ ps}^{-1}$, $g = 7.59 \cdot 10^2 \text{ ms}^{-1}$, $\gamma_r = 0.02 \text{ ps}^{-1}$, $R = 400 \text{ ms}^{-1}$, $p = 1.6$, $K_d = 0.45$ and $K_c^{(2)} = 2.5 \times 10^{-3}$. In each simulation, we determine the wavefunction $\phi(t, x)$, and extract its phase $\theta(t, x)$. We work in the low-noise regime, where the density fluctuations are negligible and topological defects are absent. In this regime the phase can be uniquely unwinded to obtain $\theta \in (-\infty, \infty)$.

KPZ scaling – We have computed the roughness function $w^2(L, t)$ for the unwinded phase θ of EP. Our results are reported in Fig. 1, and show that using the KPZ exponents, one obtains for the roughness a perfect collapse onto the expected Family-Vicsek scaling form (5). This shows that the findings of [7] obtained for appropriate parameters can also be achieved with realistic experimental conditions. Let us stress that the inclusion of a momentum-dependent damping rate is crucial since it stabilizes the solution for our choice of experimental parameters [31], which corresponds to a larger KPZ effective non-linearity parameter $|g| \equiv |\lambda|(D/2\nu^3)^{1/2} \simeq 0.48$ than that used in [7]. This difference in parameters has an important effect, since we obtain KPZ scaling not only in the long-time saturation regime $t > T_s$, where the roughness function reaches a constant in time, but also in the growth regime. If the nonlinearity is too weak, only the initial Edward-Wilkinson (EW) scaling (with $\chi = 1/2$ and $z = 2$) is visible, and the crossover to the KPZ one cannot occur before t reaches T_s .

The KPZ scaling exponents can equivalently be determined directly from the condensate wavefunction, through the first-order correlation function, $\rho_1(x, t; x', t') = \langle \phi^*(x, t)\phi(x', t') \rangle_{\xi}$. Focusing on purely spatial or purely temporal correlations, we define $C_x(x_1, x_2)|_t = -\log |\rho_1(x_1, t; x_2, t)|$ and $C_t(t_1, t_2)|_x = -\log |\rho_1(x, t_1; x, t_2)|$. At large distances, the main contribution to the correlation functions comes from the

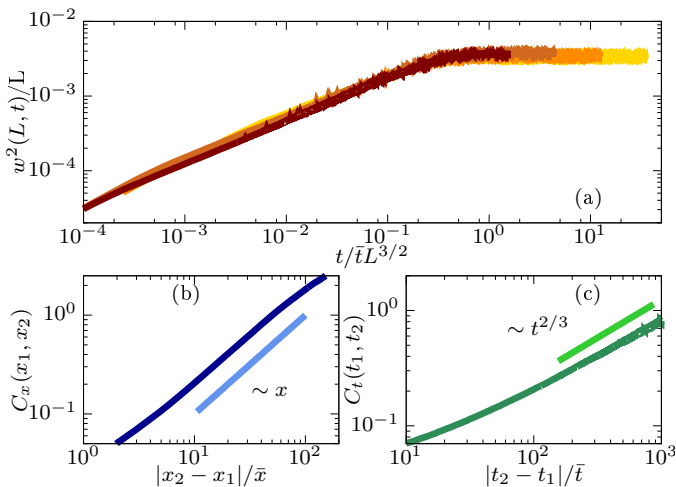


FIG. 1. (Color online) (a) Collapse of the roughness $w(L, t)$ with KPZ scaling $\chi = 1/2$, $z = 3/2$ for different system sizes $L/\bar{x} = 2^7, 2^8, 2^9, 2^{10}$ (size growing from lighter- to darker-color). Two-point (b) spatial and (c) temporal correlation together with the KPZ theoretical behavior, corresponding to a (stretched) exponential in $\rho_1(x_1, t, x_2, t) = e^{-C_x(x_1, x_2)}$ and $\rho_1(x, t_1, x, t_2) = e^{-C_t(t_1, t_2)}$

phase-phase correlations, that according to KPZ scaling should behave as $\langle \theta(x_1, t)\theta(x_2, t) \rangle \sim |x_2 - x_1|^{2\chi}$ and $\langle \theta(x, t_1)\theta(x, t_2) \rangle \sim |t_2 - t_1|^{2\beta}$ respectively. Our results for the correlation functions in the saturated regime $t > T_s$, obtained from the numerical solution of the gGPE, are shown in the lower panels of Fig. 1. For both time and space correlations, we obtain $\chi \simeq 0.49$ and $\beta \simeq 0.31$ for $L/\bar{x} = 2^{10}$ in close agreement with the KPZ exponents, which confirms our result from the roughness and validates our phase reconstruction procedure. Let us note that the time-correlation is mandatory to discriminate between the KPZ and EW scalings, since only the β exponent differs between the two in 1D. Quite remarkably, both space and time correlations are routinely experimentally accessible (see *e.g.* [32]).

Beyond scaling: Tracy-Widom statistics – As emphasized in the introduction, unprecedented theoretical advances have yielded the exact probability distribution of the fluctuations of the interface for sharp-wedge [15–17], flat [13, 14], and stationary [18, 19] initial conditions. It was shown that at long times, the interface height h behaves as $h(x, t) \simeq v_\infty t + (\Gamma t)^{1/3} \chi(x, t)$ with Γ and v_∞ non-universal parameters, and χ a random variable whose distribution is non-gaussian, and exactly given by the TW-GUE, TW-GOE or BR distribution respectively. To further assess KPZ universality in EP systems, we thus study the fluctuations of the unwinded phase $\delta\theta = (\theta - \langle \theta \rangle_{\xi, x})$ of the condensate (which subtracts the $v_\infty t$ term). In practice, we use the gGPE simulations to determine the distribution of the random variable $\tilde{\theta}(x, t) = \delta\theta/(\Gamma t)^{1/3}$, where the parameter Γ is extracted from the numerical data using the rela-

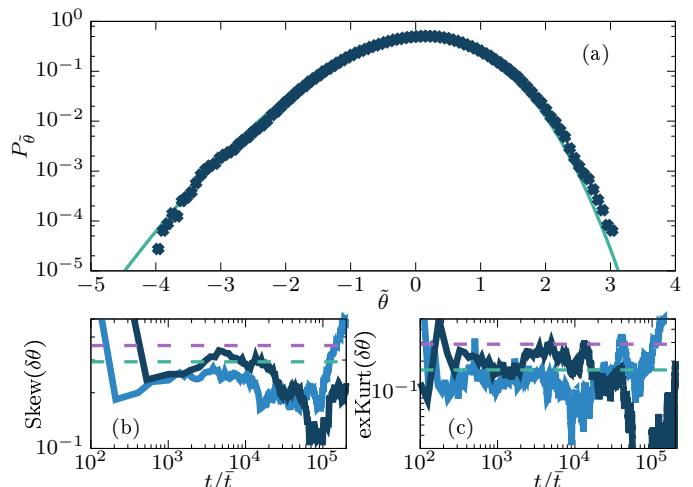


FIG. 2. (a) Distribution of $\tilde{\theta}$ for $L/\bar{x} = 2^{10}$, together with the theoretical centered GOE-TW distribution. (b) Skewness and (c) excess Kurtosis (lower panel) of the phase-field in the condensate for $L/\bar{x} = 2^9, 2^{10}$, together with the theoretical values for TW-GOE and BR statistics (green and purple dashed-line respectively). TW-GOE values are reached on a plateau around times $t/\bar{t} \simeq 10^4$.

tion $\Gamma = \lim_{t \rightarrow \infty} (\langle \delta\theta^2(x, t) \rangle / \text{Var}_\chi)^{3/2} / t$ [21, 33], with $\langle \delta\theta^2 \rangle = \langle (\theta - \langle \theta \rangle_{\xi, x})^2 \rangle_{\xi, x}$ and Var_χ is the theoretical value of the variance of the distribution. Note that since $\lambda < 0$ for the EP system, the obtained distributions for $\tilde{\theta}$ are related to $P_{-\chi}$.

To gain insight on the nature of this distribution, we first compute universal ratios of cumulants of $\delta\theta$, which do not depend on Γ , namely the skewness and the excess kurtosis, defined as $\text{Skew}(\delta\theta) = \langle \delta\theta^3 \rangle / \langle \delta\theta^2 \rangle^{3/2}$ and $\text{eKurt}(\delta\theta) = \langle \delta\theta^4 \rangle / \langle \delta\theta^2 \rangle^2 - 3$ respectively, with $\langle \delta\theta^n \rangle = \langle (\theta - \langle \theta \rangle_{\xi, x})^n \rangle_{\xi, x}$. These quantities are exactly zero for a Gaussian distribution and are known numerically at arbitrary precision for the distributions associated with the 1D KPZ equation [34, 35]. We find that they reach stationary values on plateaus depending on the system size but roughly extending between $t = 10^3$ and 10^4 in units of \bar{t} . The values of these plateaus are compatible with TW-GOE distribution (see Fig. 2-(b)). We thus used the exact value of $\text{Var}_{\text{TW-GOE}}$ to extract Γ , and recorded the probability distribution of $\tilde{\theta}$ accumulated during the plateaus, which is represented in Fig. 2-(a). We find a close agreement with the theoretical TW-GOE curve. This result provides a convincing confirmation that KPZ dynamics is relevant in EP systems. Note that the TW-GOE distribution is associated with flat (*i.e.* spatially constant) initial conditions for the θ field. This is non trivial for the phase of EP, since a transient non-universal regime exists before KPZ behavior sets in, that hinders which precise initial conditions are relevant for the associated KPZ equation.

Beyond scaling: Baik-Rains statistics – In a finite-size system, a crossover to the stationary KPZ dynamics, as-

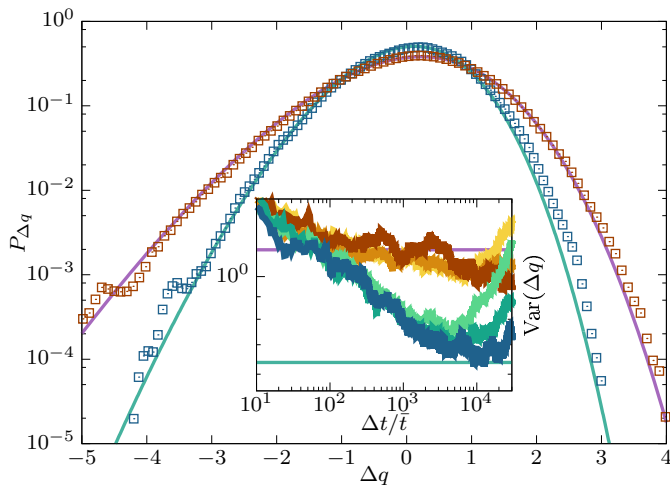


FIG. 3. (Color online) Distribution of $\Delta q(x, t_0, \Delta t)$ for $\Delta t/t_0 = 10^3$ (light-green symbols) and $\Delta t/t_0 = 5 \times 10^{-3}$ (purple symbols) for $L/\bar{x} = 2^{10}$, together with the theoretical centered TW-GOE (green solid line) and BR (purple solid line) distributions [34]. Inset (same color code): numerical and theoretical values of $\text{Var}(\Delta q)$ for different initial times $t_0/\bar{t} = 10^2, 2 \times 10^4$ (blue and brown color-scale respectively) and sizes $L/\bar{x} = 2^8, 2^9, 2^{10}$ (increasing from lighter to darker).

sociated with the Baik-Rains distribution, is expected at sufficiently long times, but before finite-size effects dominate [21]. Indications of a change are manifest in Fig. 2 since the skewness and excess Kurtosis depart from the plateaus at large times. However, this change is hindered by the noise and finite-size effects, which become more and more relevant as the correlation length becomes comparable to the system size.

In order to reduce finite-size effects and study this crossover, we follow Takeuchi [21] and introduce a new variable $\Delta q(x, t_0, \Delta t) = (\delta\theta(x, t_0 + \Delta t) - \delta\theta(x, t_0))/(\Gamma t)^{1/3}$. This variable is expected to display a TW-GOE distribution for $t_0 \rightarrow 0, \Delta t \rightarrow \infty$ and a BR distribution for $t_0 \rightarrow \infty, \Delta t \rightarrow 0$, with this precise ordering of the limits. The distribution of Δq is plotted in Fig. 3 for different ratios $\Delta t/t_0$. Both TW and BR distributions are clearly identified. Our analysis hence shows that the homogeneous EP condensate is an ideal playground to observe non-trivial out-of-equilibrium behavior associated with KPZ universality sub-classes.

Influence of the disorder – In experimental setups, the inhomogeneities due to cavity imperfections give rise to a static disorder potential. We now investigate how this affects the KPZ physics. In order to model this disorder, we introduce a random-potential $V_d(x) = |\mathcal{F}^{-1}[V_d(p)](x)|$ with $\langle V_d(x)V_d(x') \rangle = G(x - x')$, $V_d(p) = V_0 e^{i\varphi} e^{-p^2 \ell_d^2}$ and φ a uniformly distributed random-variable in the range $[0, 2\pi)$. By changing the correlation length ℓ_d , this describes any intermediate condition between a uniform potential for $\ell_d \rightarrow \infty$ to a white-noise disorder in the $\ell_d \rightarrow 0$ limit. We focus on finite values ℓ_d , corresponding

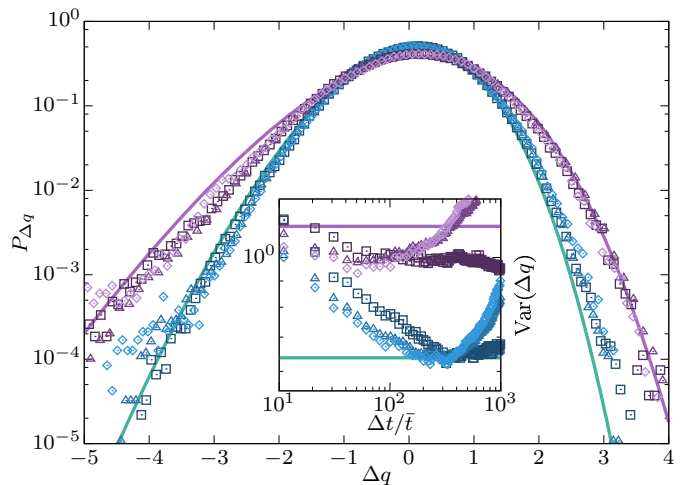


FIG. 4. (Color online) Distribution of $\Delta q(x, t_0, \Delta t)$ for different disorder correlation lengths $\ell_d/L = 0.02, 0.07, 0.15$ (from lighter to darker) for $\Delta t/t_0 \simeq 10^2$ (blue symbols) and $\Delta t/t_0 \simeq 10^{-1}$ (purple symbols), with $L/\bar{x} = 2^{10}$. The solid lines correspond to centered TW-GOE (cyan) and BR (violet) theoretical distributions [34]. Inset (same parameters and color code): numerical and theoretical values for $\text{Var}(\Delta q)$.

to a smooth disorder typical of experiments. By means of the Keldysh formalism, one can show [36] that the inclusion of a static disorder in the Keldysh action leads to a non-local shift of the KPZ noise strength. In the white-noise limit $\ell_d \rightarrow 0$ the presence of a disorder potential simply gives rise to a constant shift. However, in the case of a finite correlation length, the system is characterized by an additional microscopic length scale, which affects the phase fluctuations for times longer than the time scale $t_d \sim \ell_d^{2/3}$. We hence expect that for $t < t_d$, KPZ physics is still observable, while for $t > t_d$ the features of the disorder become dominant. The roughness and correlation functions computed in presence of the disorder indeed confirm this picture [36]. We determined the distribution of the variable Δq , in both regimes of large and small $\Delta t/t_0$. The results, presented in Fig. 4, show that for large $\Delta t/t_0$, the TW-GOE distribution is still accurately reproduced. Increasing t_0 , the approach to the BR distribution is also clearly visible, even if it cannot be fully attained, since t_0 is limited to t_d by the presence of the disorder.

Conclusion – We have shown that universal KPZ physics can be observed under realistic experimental conditions in the dynamics of the phase of one-dimensional exciton polaritons. Our analysis shows that the roughness function, the first-order correlation functions and the probability distributions of the phase fluctuations display universal KPZ features, such as a time stretched exponential decay of correlations and non-Gaussian probability distributions. We evidenced in particular a crossover between TW-GOE and BR statistics, allowing to probe two well-known sub-classes of 1D KPZ universality. Furthermore,

we have shown that the presence of a static disorder does not destroy KPZ physics on sufficiently small timescales. This analysis suggests new experimental protocols for the observation of KPZ properties in exciton-polaritons.

The authors would like to thank Dario Ballarini, Denis Basko, Maxime Richard and Alberto Rosso for inspiring discussions on both theoretical and experimental aspects. This work is supported by French state funds ANR-10-LABX-51-01 (Labex LANEF du Programme d'Investissements d'Avenir) and CNRS through grant Infinity NEQ-DYN.

-
- [1] M. Kardar, G. Parisi, and Y.-C. Zhang, *Phys. Rev. Lett.* **56**, 889 (1986).
- [2] T. Halpin-Healy and Y.-C. Zhang, *Physics Reports* **254**, 215 (1995).
- [3] J. Krug, *Adv. Phys.* **46**, 139 (1997).
- [4] I. Corwin, *Random Matrices: Theory and Applications* **01**, 1130001 (2012).
- [5] K. Ji, V. N. Gladilin, and M. Wouters, *Phys. Rev. B* **91**, 045301 (2015).
- [6] V. N. Gladilin, K. Ji, and M. Wouters, *Phys. Rev. A* **90**, 023615 (2014).
- [7] L. He, L. M. Sieberer, E. Altman, and S. Diehl, *Phys. Rev. B* **92**, 155307 (2015).
- [8] E. Altman, L. M. Sieberer, L. Chen, S. Diehl, and J. Toner, *Phys. Rev. X* **5**, 011017 (2015).
- [9] M. Wouters and V. Savona, *Phys. Rev. B* **79**, 165302 (2009).
- [10] L. M. Sieberer, M. Buchhold, and S. Diehl, *Reports on Progress in Physics* **79**, 096001 (2016).
- [11] I. Carusotto and C. Ciuti, *Rev. Mod. Phys.* **85**, 299 (2013).
- [12] C. Tracy and H. Widom, *Commun. Math. Phys.* **159**, 151 (1994).
- [13] P. Calabrese and P. Le Doussal, *Phys. Rev. Lett.* **106**, 250603 (2011).
- [14] P. Calabrese and P. Le Doussal, *J. Stat. Mech.* P06001 (2012).
- [15] G. Amir, I. Corwin, and J. Quastel, *Commun. Pure Appl. Math.* **64**, 466 (2011).
- [16] T. Sasamoto and H. Spohn, *Nucl. Phys. B* **834**, 523 (2010).
- [17] P. Calabrese, P. L. Doussal, and A. Rosso, *EPL (Europhysics Letters)* **90**, 20002 (2010).
- [18] T. Imamura and T. Sasamoto, *Phys. Rev. Lett.* **108**, 190603 (2012).
- [19] T. Imamura and T. Sasamoto, *Journal of Statistical Physics* **150**, 908 (2013).
- [20] K. A. Takeuchi and M. Sano, *Phys. Rev. Lett.* **104**, 230601 (2010).
- [21] K. Takeuchi and M. Sano, *J. Stat. Phys.* **147**, 853 (2012).
- [22] J. ichi Wakita, H. Itoh, T. Matsuyama, and M. Matsushita, *Journal of the Physical Society of Japan* **66**, 67 (1997).
- [23] J. Maunuksela, M. Myllys, O.-P. Kähkönen, J. Timonen, N. Provatas, M. J. Alava, and T. Ala-Nissila, *Phys. Rev. Lett.* **79**, 1515 (1997).
- [24] K. A. Takeuchi, *Phys. Rev. Lett.* **110**, 210604 (2013).
- [25] M. Wouters and I. Carusotto, *Phys. Rev. Lett.* **99**, 140402 (2007).
- [26] C. Ciuti, G. Bastard, and I. Carusotto, *Phys. Rev. B* **72**, 115303 (2005).
- [27] M. Wouters and V. Savona, *Phys. Rev. B* **79**, 165302 (2009).
- [28] F. Family and T. Vicsek, *Journal of Physics A: Mathematical and General* **18**, L75 (1985).
- [29] M. Werner and P. Drummond, *Journal of Computational Physics* **132**, 312 (1997).
- [30] G. R. Dennis, J. J. Hope, and M. T. Johnsson, *Computer Physics Communications* **184**, 201 (2013).
- [31] Note that a similar imaginary diffusion constant was introduced in [7] on an argument of relevance in the renormalization group sense, to stabilize the simulation.
- [32] A. Trichet, E. Durupt, F. Médard, S. Datta, A. Minguzzi, and M. Richard, *Phys. Rev. B* **88**, 121407 (2013).
- [33] T. Halpin-Healy and Y. Lin, *Phys. Rev. E* **89**, 010103 (2014).
- [34] M. Prähofer and H. Spohn, *Phys. Rev. Lett.* **84**, 4882 (2000).
- [35] F. Bornemann, *Mathematics of Computation* **79**, 871 (2010).
- [36] D. Squizzato, L. Canet, and A. Minguzzi, in preparation (2017).